Hind foot drumming: Volumetric micro-computed tomography investigation of the hind limb musculature of three African mole-rat species (Bathyergidae)

L. Sahd[1], N.C. Bennett[2], S.H. Kotzé[1,3]

[1] Division of Clinical Anatomy, Department of Biomedical Sciences, Faculty of Medicine and Health Sciences, Stellenbosch University, Cape Town 8000, South Africa
[2] Department of Zoology and Entomology, Mammal Research Institute, University of Pretoria, Pretoria 0002, South Africa
[3] Department of Biomedical Sciences, Ross University School of Veterinary Medicine, Basseterre, St Kitts and Nevis, West Indies

Running Title: Digital myology of African mole-rats
Editorial correspondence:
Prof S.H. Kotzé
Postal address: Department of Biomedical Sciences, Faculty of Medicine and Health Sciences, Stellenbosch University, PO Box 241, Cape Town, South Africa
Email: shk@sun.ac.za

Funding information:
National Research Foundation (NRF; Grant number: 120827) and SARChi Mammal Behavioural Ecology and Physiology (Grant number 64756)

Data availability statements:
The data that support the findings of this study are available from the corresponding author upon reasonable request.
The unanalysed diceCT scans will be available from Lauren Sahd upon reasonable request
Email:lauren.sahd22@gmail.com

Conflict of interest:
The authors have no conflict of interest to declare.

ABSTRACT
Several species of African mole-rats use seismic signalling by means of hind foot drumming for communication. The present study aimed to create three-dimensional reconstructions and compare volumetric measurements of 27 muscles of the hind limb of two drumming (*Georychus capensis* and *Bathyergus suillus*) and one non-drumming (*Cryptomys hottentotus natalensis*) species of African mole-rats. Diffusible iodine contrast-enhanced micro-computed tomography (diceCT) scans were performed on six specimens per species. Manual segmentation of the scans using VGMAX Studio imaging software allowed for individual muscles to be separated while automatically determining the volume of each muscle. The volume of the individual muscles was expressed as a percentage of the total hind limb volume and statistically compared between species. Subsequently, three-dimensional reconstructions of these muscles were created. *Musculus gracilis anticus* had a significantly larger percentage of the total hind limb muscle volume in both drumming species compared to the non-drumming *C. h. natalensis.* Furthermore, several hip and knee extensors, namely *mm. gluteus superficialis*, *semimembranosus, gluteofemoralis*, *rectus femoris*

and *vastus lateralis,* had significantly larger muscle volume percentages in the two drumming species (*G. capensis* and *B. suillus*) compared to the non-drumming species. While not statistically significant, *G. capensis* had larger muscle volume percentages in several key hip and knee extensors compared to *B. suillus.* Additionally*, G capensis* had the largest summed percentage of the total hind limb volume in the hip flexor, hip extensor, knee extensor and ankle plantar flexor muscle groups in all the three species. This could be indicative of whole muscle hypertrophy in these muscles due to fast eccentric contractions that occur during hind foot drumming. However, significantly larger muscle volume percentages were observed in the scratch digging *B. suillus* compared to the other two chisel tooth digging species. Moreover, while not statistically significant, *B. suillus* had larger muscle volume percentages in several hip extensor and knee flexor muscles compared to *G. capensis* (except for *m. vastus lateralis*)*.* These differences could be due to the large relative size of this species but could also be influenced by the scratch digging strategy employed by *B. suillus*. Therefore, while the action of hind foot drumming seems to influence certain key muscle volumes, digging strategy and body size may also play a role.

Key words: Hind limb; diceCT, Seismic signalling; Muscle volume

INTRODUCTION

African mole-rats (Bathyergidae) are a family of subterranean rodents endemic to many different habitats across the southern Saharan African continent (Bennett & Faulkes, 2000). These subterranean rodents rarely leave their burrow systems (Nowack & Paradiso, 1983; Sherman, et al.*,* 1991; Bennett, et al., 1993; Bennett*.* et al*,* 2006) and several species use hind foot drumming to generate seismic signals as a means of communication to hetero- and conspecifics. Hind foot drumming has been extensively studied in the chisel-tooth digging Cape mole-rat (*Georychus capensis*; Pallas, 1778). This species starts drumming as early as 50 days after birth and uses drumming in both territorial and courtship displays. Males drum at a rate of 26 beats per second and females drum at the relatively slower rate of 15 beats per second during the mating season (Bennett & Jarvis, 1988, Narins, et al., 1992; Bennett & Faulkes, 2000; Van Sandwyk & Bennett, 2005). While no actual rate of drumming has been reported, the Cape dune mole-rat (*Bathyergus suillus*; Schreber, 1782), a scratch digger, starts drumming around 80 days after birth. They use hind foot drumming for territorial displays and during their courtship ritual where the pair will drum to each other with increasing frequency and speed (Bennett & Faulkes, 2000; Hart., et al 2006). Hind foot drumming has not been reported in the chisel-tooth digging Natal mole-rat (*Cryptomys hottentotus natalensis*; Roberts, 1913), but anecdotal observations of a foot thump in other sub-species *of C. hottentotus* have been reported (Lacey, et al., 2000). However, while it is not certain if these occasional thumps are seismic signals (Mason & Narins, 2010), they are not regarded as hind foot drumming.

While the context and behaviour of drumming in these species have been well documented, few studies have determined the morphological adaptations for this behaviour. Sahd et al. (2019), documented that the *m. gracilis* complex (*mm. gracilis anticus and posticus*) was the only macroscopic morphological difference between the drumming and non-drumming species. *Georychus capensis and B. suillius* both had a single *m. gracilis* while *C. h. natalensis* had both parts of the *m. gracilis*. Further investigations by Sahd et al. (2021) suggested that *m. gracilis anticus* may potentially play a key role in hind foot drumming as it was the only muscle to have statistically significant larger values in *G. capensis* compared to *C. h. natalensis* in all muscle architecture parameters (L_f, M_M, PCSA) analysed. Sahd et al.(2021) found that the hip extensors and knee flexors of both the drumming species (*G. capensis* and *B. suillus*) were shown to be capable of higher power output (fast and forceful contraction) compared to the non-drumming species.

Micro-computed tomography (CT) scanning is becoming a common technique in the study of comparative morphology. The further development of diffused iodine contrast-enhanced micro-computed tomography (diceCT) scanning has enabled soft tissue, and specifically muscles, to be studied in more detail (Jeffery, et al., 2011). This contrast enhanced scanning has allowed for a non-destructive analysis of small specimens that would otherwise not be able to be studied in much detail (Metchser, 2009; Vickerton, et al., 2013). Charles, et al. (2016) used diceCT scanning to digitally dissect the hind limb of the mouse and determine its muscle architecture parameters. Additionally, diceCT scanning has been used to digitally dissect the masticatory and facial muscles of several primate species including the blue-eyed black lemur (*Eulemur flavifrons*; Dickinson, et al., 2020a), the common marmoset (*Callithrix jacchus*; Dickinson, et al., 2019) and the Aye-Aye (*Daubentonia madagascariensis*; Dickinson, et al., 2020b). Several studies have comparatively studied the masticatory musculature of African mole-rats (Bathyergidae; Cox & Faulkes, 2014; Cox, et al., 2020), bats (Santana, 2018) and anteaters (Ferreira-Cardoso, et al., 2020), however no statistical analysis comparing the species was performed in these studies as they compared only one individual per species. Locomotory studies on the limbs of crocodilians (Klinkhamer, et al., 2017; Wiseman, et al., 2021), frogs (Collings & Richards, 2019) and birds (Sullivan, et al., 2019; Bishop, et al., 2021) have also employed diceCT scanning.

In hind foot drumming bathyergid species, the drumming action is achieved by rapid flexion and extension of the hip and knee joints of either a single or alternating hind limb (Randall, 2014). The aim of the present study was to create three dimensional (3-D) reconstructions from diceCT scans of the hind limb musculature of drumming and non-drumming African mole-rats to determine if there were differences in volumetric muscle measurements between the studied species. Additionally, based on muscle architecture differences observed between the drumming and non-drumming mole-rat species studied here (Sahd, et al., 2021), the present study hypothesised that the hip and knee extensors of two drumming species (*G. capensis* and *B, suillus*) would have a higher percentage volume of the total hind limb muscle volume compared to a non-drumming species (*C. h. natalensis*). Furthermore, it was hypothesized the ankle dorsi-and plantar flexors of the three species studied here would have similar percentage volumes of the total hind limb muscle volume.

MATERIALS AND METHODS

Samples

One formalin fixed hind limb of 18 animals, consisting of three species, were obtained from unrelated previously ethically cleared studies (Table 1). This included *G. capensis* (the Cape mole-rat; n=6), *B. suillus* (the Cape-dune mole-rat; n=6) and *C. h. natalensis* (the Natal mole-rat; n=6). Ethical approval for the use of the specimens was obtained from the Stellenbosch University Research Ethics Committee: Animal Care and Use (SU-ACUM 16-00005) and the Animal Ethics Committee of the University of

Pretoria EC079-17. Each specimen was stained in a 3.75% (w/v %) iodine potassium iodide (I_2KI) aqueous solution (Metscher, 2009; Degenhardt & Wright, 2010; Jeffery et al., 2011; Gignac et al., 2016) for one (*C. h. natalensis*), two (*G. capensis*) and four (*B. suillus*) weeks respectively (based on the size of the sample) to increase the contrast of the soft tissue. The solution was agitated daily and refreshed weekly. Specimens were protected from sunlight during staining to prevent weakening the potency of the I_2KI solution (Gignac et al., 2016).

Table 1 Species information including ethical clearance, capture site, mean hind limb volume and mean body mass.

Species	Ethical approval	n	Capture site	Mean hind limb volume (mm^3)	Mean body mass (g)
Georychus capensis	University of Johannesburg: 215086650-10/09/15	6	Darling, Western Cape	14 349.45 ± 3 951.59	210.56 ± 30.80
Bathyergus suillus	Stellenbosch University: 10NP_VAN01	6	Darling, Western Cape	85 887.14 ± 17 598.57	730 ± 161
Cryptomys hottentotus natalensis	University of Pretoria: ECO0070-14	6	Glengarry, Kwa-Zulu Natal	9 263.23 ± 3 414.04	121.8 ± 26.47

Determination of staining duration

Feasibility tests to determine the best staining procedure were conducted on a *G. capensis* sample as representative of all three species. Micro-CT scans were taken at various staining intervals to determine the best staining duration that provides the best contrast of the soft tissue. A scan of a non-stained specimen was performed as a reference point, whereafter scans of samples stained for one day, one week and 2 weeks were completed respectively (Figure 1). The specimen was also tested for staining with the skin still intact (Figure 1 A-C) and the skin removed (Figure 1 D). The results of the feasibility test indicated that staining the specimen with the skin removed and for 2 weeks provided the most detail of the individual muscles. Due to the size differences between the species, it was estimated that the smaller *C. h. natalensis* samples would be stained for half the duration i.e., one week and that the large *B. suillus samples* would be stained for double the duration i.e., 4 weeks.

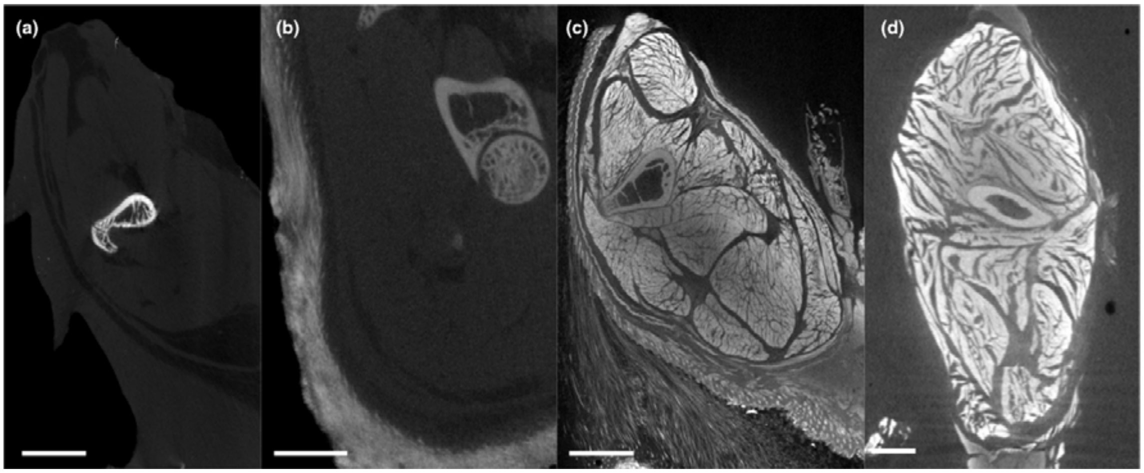

Figure 1 *Georychus capensis* coronal slices with differing staining durations using a 3.75% I_2KI aqueous solution. A) unstained with skin intact, bar =6 mm. B) one day of staining with skin intact, bar =3.5 mm. C) staining for seven days, skin intact, bar = 4 mm. D) stained for 14 days, skin removed, bar= 3.5 mm.

Scanning and segmentation

The hind limbs were scanned using diceCT scanning at the CT facility (du Plessis, et al., 2016) of the Central Analytical Facility (CAF) of Stellenbosch University in Stellenbosch using a General Electric VTomex L240 micro-CT Scanner (*General Electric Sensing and Inspection Technologies/Phoenix X-ray, Wunstorff, Germany*). Each scan was done for a duration of 45 minutes with the following scanning parameters: a voltage of 150 kilovolts (kv) and an amplitude of 200 microamps (µA) with the addition of a 0.5 mm copper filter and a voxel size of 0.055 mm. One additional scan per species was conducted prior to staining, to obtain images of the hind limb bones. The projections were reconstructed with a beam hardening algorithm applied (pre-set at level 8) in phoenixdatos|x CT data Acquisition software (*Waygate Technologies, Hürth, Germany*).

Volumetric measurements of 27 individual muscles (as identified by the description in Sahd, et al., 2019) were made using manual segmentation (Figure 2) with Volume Graphics VGStudioMax 3.4 (*Volume Graphics, Heidelberg, Germany*) software. If a muscle did not have distinct borders throughout the whole scan, the muscle was excluded, as was the case with *mm. iliacus* and *psoas major* in all *B. suillus* samples. Muscle volumes obtained were corrected for fixation and staining shrinkage by an increase of 41.6% in all samples studied (Buytaert, et al., 2014). To allow for comparisons of muscle volume between species, each individual muscle volume was expressed as a percentage of the total hind limb muscle volume. This was done to compensate for the size difference between species. Individual muscle volumes were obtained from the micro-CT scans using image segmentation and selection. The images obtained from the micro-CT scans were used to reconstruct 3-D illustrations of the muscles of the hind limbs.

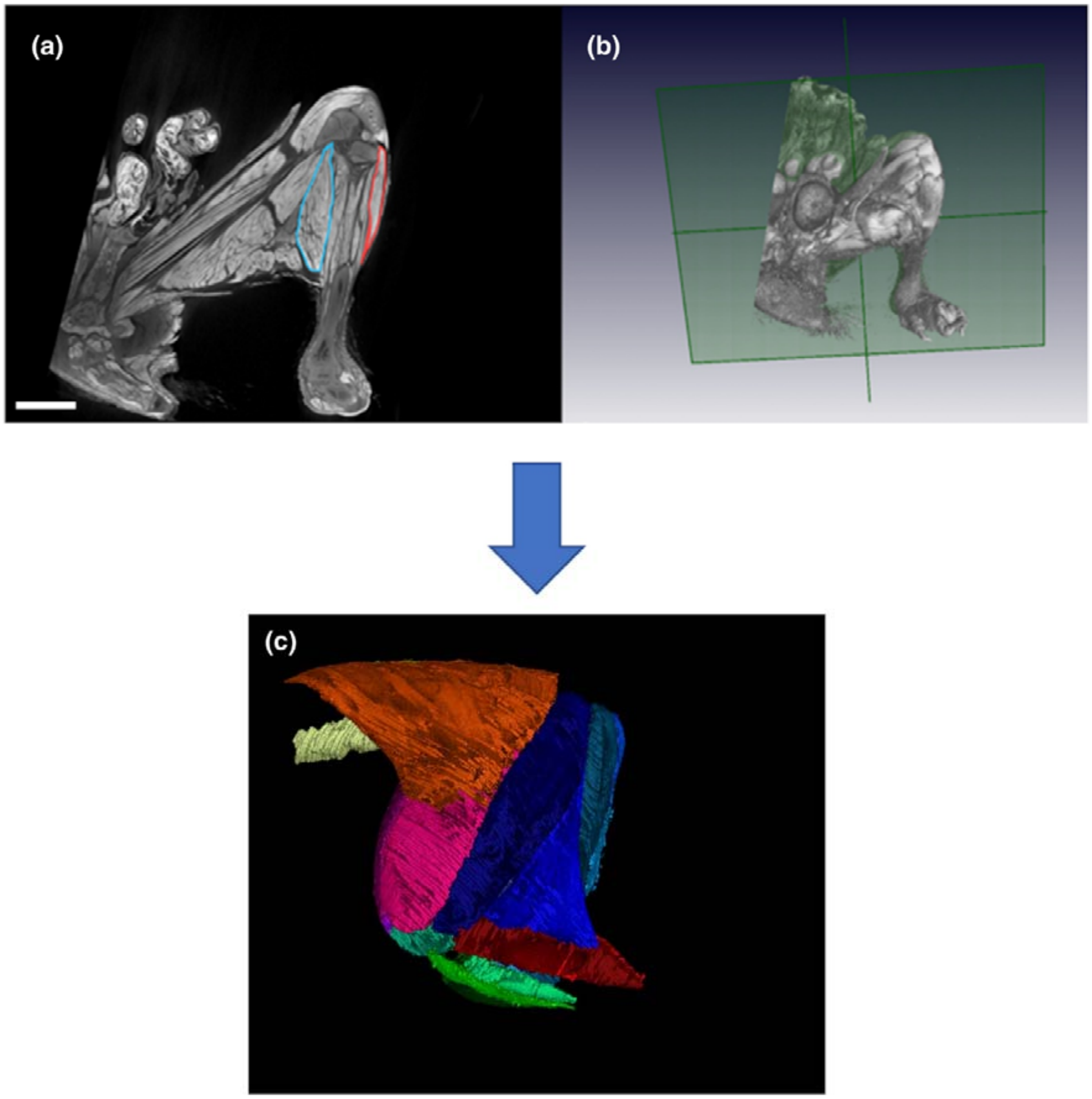

Figure 2 Workflow from manual segmentation of the muscles from the 2-D slices to the individually segmented muscles in a 3-D rendering. A) The 2-D slice of micro-CT scan with blue and red outlines indicating muscles that have been segmented, bar= 7 mm. B) 3-D rendering of the sample to indicate the position within the sample. C) 3-D rendering of the segmented muscles.

Statistical analysis

Descriptive statistics including the mean and standard deviation were reported per species. One-way analysis of variance (ANOVA) was used to determine significant differences between species. Fischer's Least Significant Difference (LSD) *post-hoc* test was used to determine p-values. Statistically significant results were determined with a $p < .05$. All statistical analysis was performed using R (R core team, 2013; RRID:SCR_001905). Graphs were created in ggplot2 (Wickham, 2016; RRID:SCR_014601) in R (R core team, 2013).

RESULTS

The micro-CT scans confirmed an observation from Sahd et al. (2019) of a single *m. gracilis* in *Georychus capensis* and *Bathyergus suilus* (Figure 3).

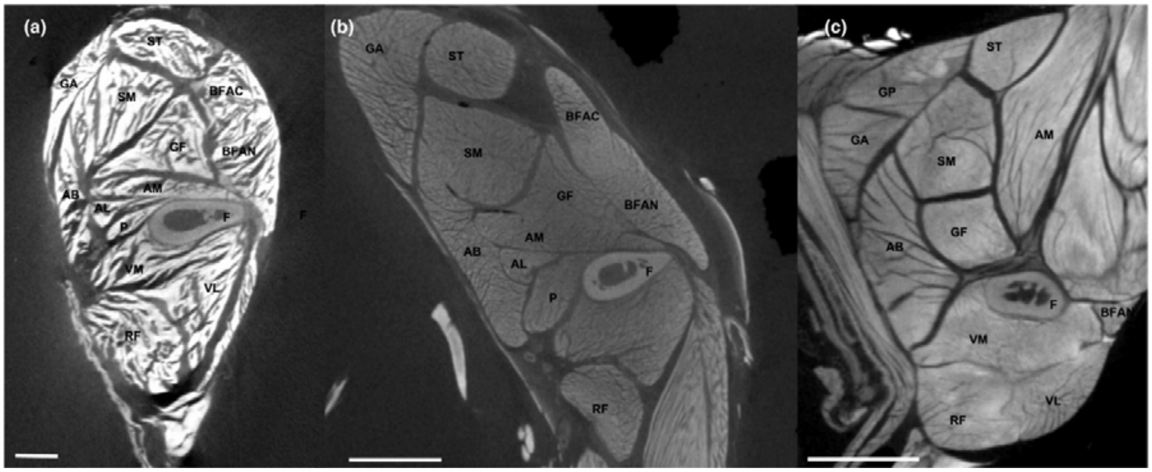

Figure 3 Coronal section of the mid-thigh in *Georychus capensis* (A), *Bathyergus suillus* (B), and *Cryptomys hottentotus natalensis* (C) showing the single *m. gracilis* in the two drumming species (A & B) and the double *m. gracilis* (*mm. gracilis anticus* and *gracilis posticus*) in the non-drumming species (C). A).*Georychus capensis* bar =2.5 mm. B) *Bathyergus suillus* bar=6.5 mm. C) *Cryptomys hottentotus natalensis* bar=3 mm. Muscle abbreviations: *m. adductor brevis* (AB), *m. adductor longus* (AL), *m. adductor magnus* (AM), *m. biceps femoris* cranial head (BFAN), *m. biceps femoris* caudal head (BFAC), *m. gluteofemoralis* (GF), *m. gracilis anticus* (GA), *m. gracilis posticus*, *m. gracilis posticus* (GP), *m. pectineus* (P), *m. rectus femoris* (RF) *m. semimembranosus* (SM), *m. semitendinosus* (ST), *m. vastus lateralis* (VL), *m. vastus medialis* (VM). Femur (F).

Three-dimensional reconstructions of hind limb

The 3-D reconstructions of the hind limbs of *G. capensis* and *C. h. natalensis* are depicted in Figures 4 and 5.

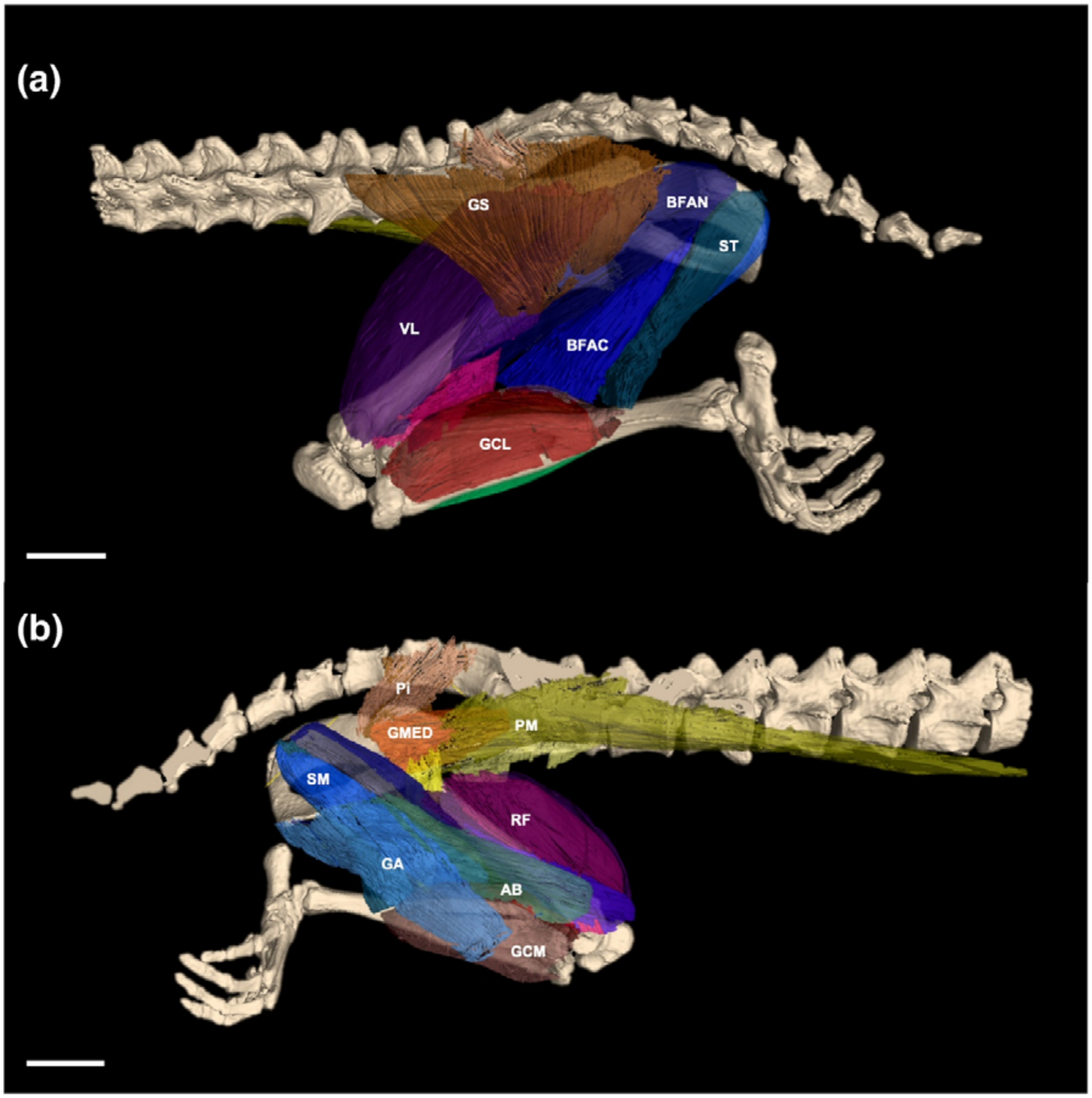

Figure 4. The lateral (A) and medial view (B) of the left hind limb of *Georychus capensis* as a representative sample of the two drumming species. The medial view has been angled to the best position for display of the muscles. Muscle abbreviations*: m. adductor brevis* (AB), *m. biceps femoris* cranial head (BFAN), *m. biceps femoris* caudal head (BFAC), *m. gracilis anticus* (GA), *m. gastrocnemius* lateral head (GCL), *m. gastrocnemius* medial head (GCM), *m. gluteus medius* (GMED), *m. gluteus superficialis* (GS), *m. piriformis* (PI), *m. psoas major* (PM), *m. rectus femoris* (RF), *m. semimembranosus* (SM), *m. semitendinosus* (ST), *m. vastus lateralis* (VL). Bar = 5 mm.

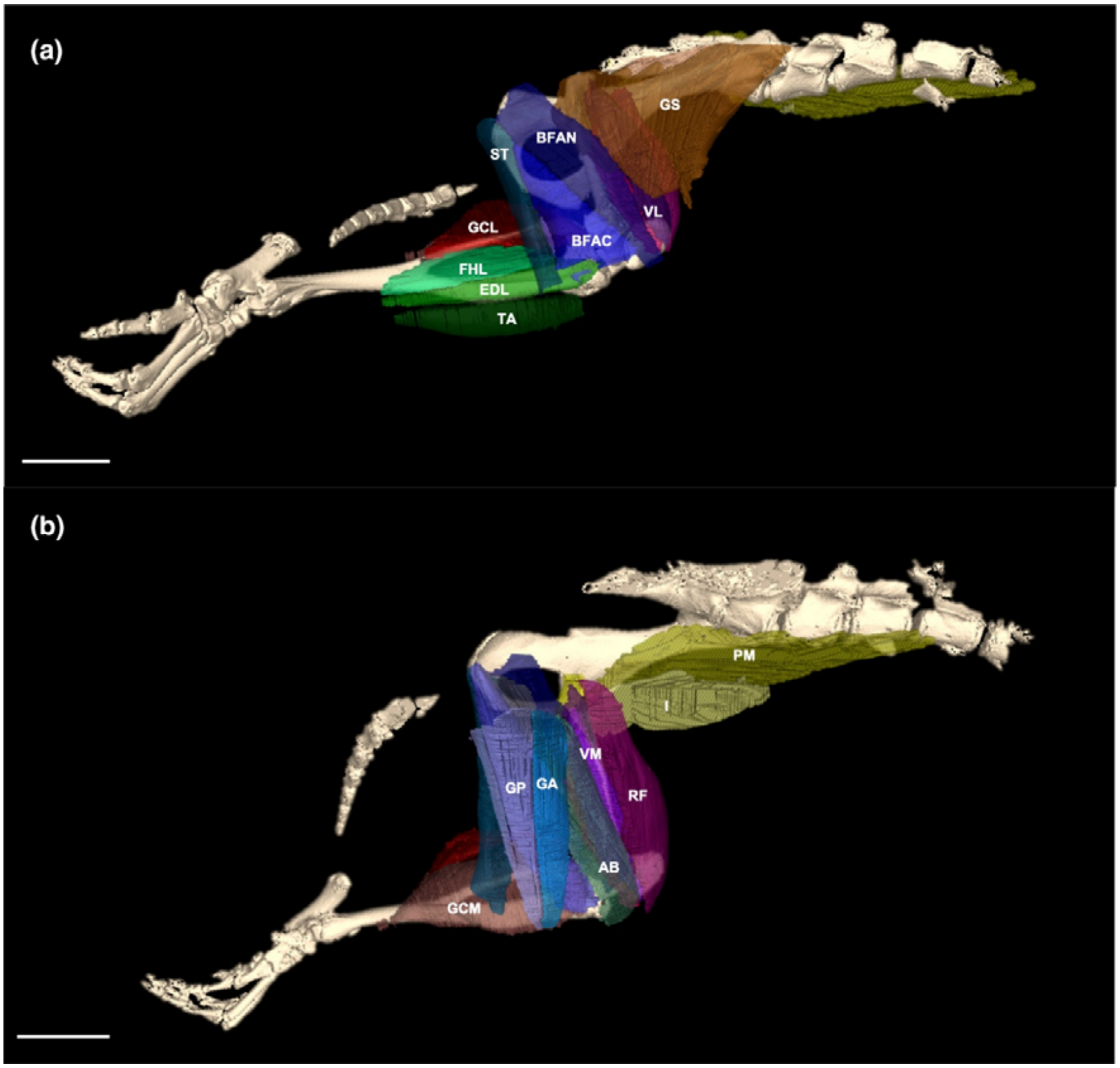

Figure 5 The lateral (A) and medial view (B) of the right hind limb of the non-drumming *Cryptomys hottentotus natalensis*. The medial view has been angled to the best position to demonstrate the muscles. Muscle abbreviations*: m. adductor brevis* (AB), *m. biceps femoris* cranial head (BFAN), *m. biceps femoris* caudal head (BFAC), *m. extensor digitorum longus* (EDL), *m. flexor hallucis longus* (FHL), *m. gracilis anticus* (GA), *m. gracilis posticus* (GP), *m. gastrocnemius* lateral head (GCL), *m. gastrocnemius* medial head (GCM), *m. gluteus superficialis* (GS), *m. illiacus* (I), *m. piriformis* (PI), *m. psoas major* (PM), *m. rectus femoris* (RF), *m. semimembranosus* (SM), *m. semitendinosus* (ST), *m. tibialis cranialis* (TA), *m. vastus lateralis* (VL), *m. vastus medialis* (VM). Bar = 5 mm.

Volumetric measurements

The mean volume of the individual muscles for each species is detailed in Table 2. The mean muscle volume of each muscle expressed as a percentage of the total hind limb muscle volume is illustrated in Figure 6. The mean summed percentage muscle volume of each functional muscle group (Table 3) is seen in Figure 7.

Table 2 Mean and standard deviation of the individual muscle volumes (mm^3) obtained per species.

Muscle	*Georychus capensis*	*Bathyergus suillus*	*Cryptomys hottentotus natalensis*
Adductor brevis	249.96 ± 87.92	1406.78 ± 524.96	115.73 ± 64.35
Adductor longus	43.77 ± 34.28	266.23 ± 84.16	21.44 ± 6.41
Adductor magnus	163.22 ± 88.99	1737.43 ± 602.67	101.70 ± 41.26
Biceps femoris cranial head	333.86 ± 60.07	1864.88 ± 452.79	131.75 ± 48.05
Biceps femoris caudal head	168.69 ± 24.54	929.34 ± 290.37	103.32 ± 33.79
Extensor digitorum longus	36.40 ± 10.48	310.76 ± 53.40	19.90 ± 7.21
Flexor hallucis longus	34.43 ± 12.62	296.41 ± 89.57	15.31 ± 12.71
Gracilis anticus	229.92 ± 98.50	2473.59 ± 603.09	53.62 ± 14.47
Gastrocnemius medial head	146.28 ± 19.05	581.62 ± 228.24	66.58 ± 22.91
Gastrocnemius lateral head	158.19 ± 20.72	702.63 ± 73.52	64.56 ± 18.35
Gluteofemoralis	236.42 ± 41.79	1563.91 ± 289.35	67.18 ± 25.44
Gluteus medius	237.16 ± 103.20	1851.53 ± 732.40	70.15 ± 18.87
Gracilis posticus	-	-	62.72 ± 25.89
Gluteus superficialis	318.69 ± 84.97	2276.48 ± 250.74	111.97 ± 44.68
Iliacus	199.29 ± 75.12	-	59.75 ± 22.82
Pectineus	42.27 ± 24.58	344.71 ± 112.73	19.12 ± 11.78
Piriformis	112.81 ± 84.42	970.58 ± 379.97	76.68 ± 31.84
Plantaris	71.01 ± 23.65	303.26 ± 67.08	36.73 ± 16.99
Psoas major	227.77 ± 62.65	-	78.22 ± 73.44
Rectus femoris	294.64 ± 79.12	2030.65 ± 666.63	139.48 ± 64.13
Soleus	13.98 ± 7.09	218.43 ± 96.72	14.27 ± 5.21
Semimembranosus	420.01 ± 91.83	3243.85 ± 665.78	155.94 ± 65.48
Semitendinosus	220.94 ± 33.05	1215.09 ± 196.04	101.37 ± 32.88
Tibialis cranialis	97.60 ± 18.91	629.13 ± 157.17	54.29 ± 16.23
Vastus intermedius	108.29 ± 38.58	520.73 ± 164.90	47.83± 25.09
Vastus medialis	141.83 ± 45.33	604.40 ± 232.57	52.43 ± 22.85
Vastus lateralis	444.17 ± 153.06	2332.93 ± 601.18	140.69 ± 72.04

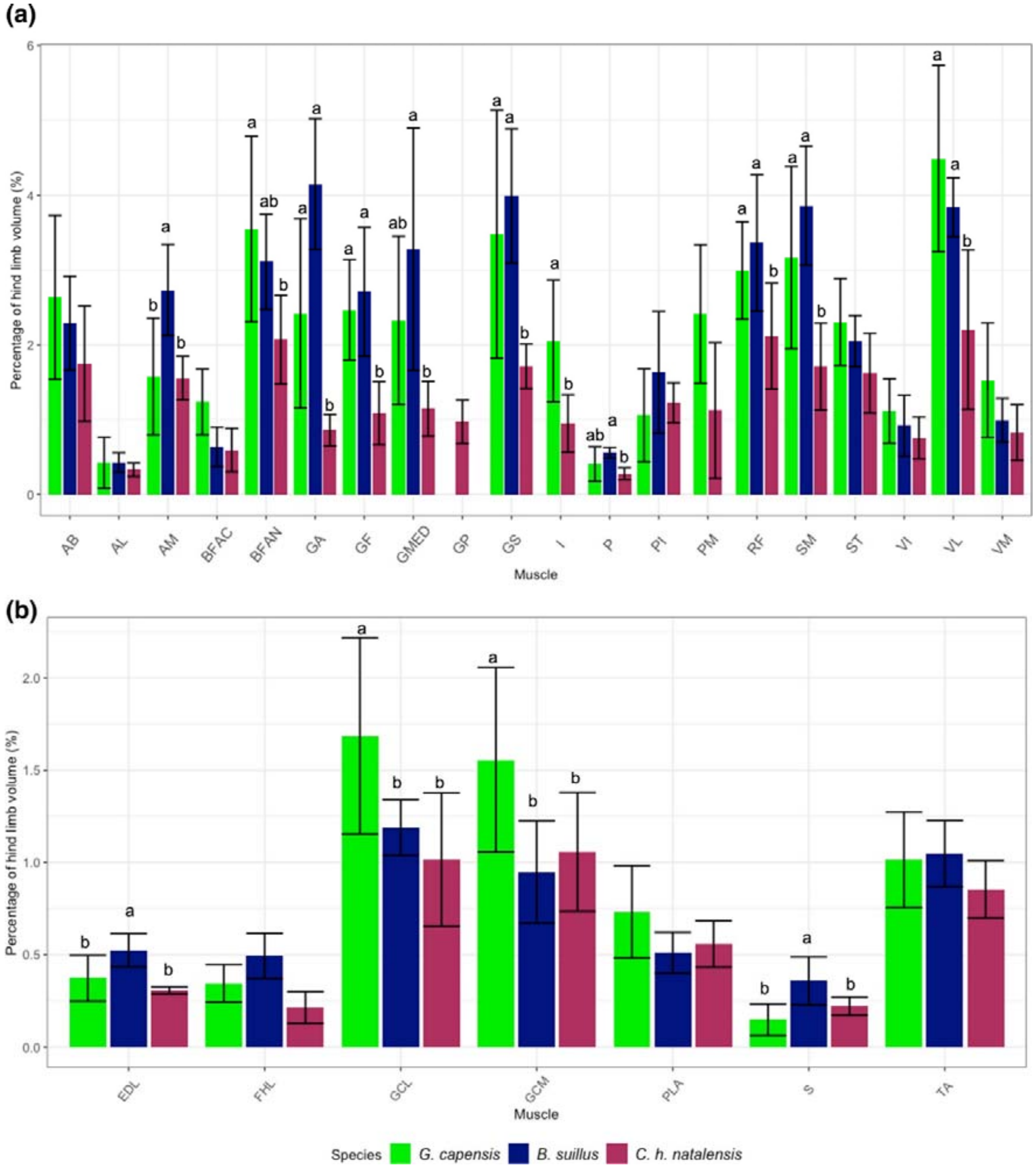

Figure 6 The mean percentage of the total hind limb per muscle for *Georychus capensis, Bathyergus suillus* and *Cryptomys hottentotus natalensis*. The error bars indicate the standard deviation. A) The proximal muscles and B) the distal muscles. Muscle abbreviations: *m. adductor brevis* (AB),*m. adductor longus* (AL), *m. adductor magnus* (AM), *m. biceps femoris* cranial head (BFAN), *m. biceps femoris* caudal head (BFAC), *m. extensor digitorum longus* (EDL), *m. flexor hallucis longus* (FHL), *m. gracilis anticus* (GA), *m. gracilis posticus* (GP), *m. gastrocnemius* lateral head (GCL), *m. gastrocnemius* medial head (GCM), *m. gluteofemoralis* (GF), *m. gluteus medius* (GMED), *m. gluteus superficialis* (GS), *m. ililacus* (I), *m. pectineus* (P), *m. piriformis* (PI), *m. plantaris* (PLA), *m. psoas major* (PM), *m. rectus femoris* (RF), *m. soleus* (S), *m. semimembranosus* (SM), *m. semitendinosus* (ST), *m. tibialis cranialis* (TA), *m. vastus intermedius* (VI), *m. vastus lateralis* (VL), *m. vastus medialis* (VM).

Table 3 The functional muscle groups of the hind limb muscles. Bi-articular muscle will appear in more than one muscle group.

Hip flexors (HF)	*M. iliacus* *M. psoas major* *M. pectineus* *M. rectus femoris*
Hip extensors (HE)	*M. gluteus superficialis* *M. gluteus medius* *M. semitendinosus* *M. biceps femoris* *M. semimembranosus* *M. gluteofemoralis*
Hip rotators (Studied as an individual muscle)	*M. piriformis*
Hip adductors (HA)	*M. adductor brevis* *M. gracilis anticus* *M. gracilis posticus* (only in *C .h. natalensis*) *M. adductor longus* *M. adductor magnus*
Knee extensors (KE)	*M. vastus lateralis* *M. vastus medialis* *M. vastus intermedius* *M. rectus femoris*
Knee flexors (KF)	*M. semitendinosus* *M. biceps femoris* *M. semimembranosus* *M. gracilis anticus* *M. adductor longus* *M. gastrocnemius* *M. plantaris*
Ankle dorsiflexors (ADF)	*M. tibialis cranialis* *M. extensor digitorum longus*
Ankle plantar flexors (APF)	*M. gastrocnemius* *M. soleus* *M. plantaris* *M. flexor hallucis longus*

The two drumming species (*G. capensis* and *B. suillus*) had significantly larger muscle volume percentages compared to the non-drumming species in several hip and knee flexors and extensors. This included *mm. gluteus superficialis* (F=6.283 p<0.01), *semimembranosus* (F=9.122, p<0.01), *gluteofemoralis* (F=12.716, p<0.01), *rectus femoris* (F=6.569, p<0.01) and *vastus lateralis* (F=11,268, p<0.01). Additionally, *m. gracilis anticus* had significantly larger muscle volume percentages in the two drumming species compared to *C. h. natalensis* (F=19.745, p<0.01).

Bathyergus suillus had significantly larger muscle volume percentages in *mm. gluteus medius* (F=4.468, p=0.04) and *pectineus* (F=4.319, p=0.04) compared to *C. h. natalensis.* Furthermore, *G. capensis* had significantly larger muscle volume percentages in the cranial head of *m. biceps femoris* (F=5.004, p=0.02) and *m. iliacus* (F=5.406, p=0.03) than *C. h. natalensis*.

Bathyergus suillus had significantly larger muscle volume percentages in *mm. adductor magnus* (F=5.663 p=0.02), *extensor digitorum longus* (F=8.916 p<0.01) and soleus (F=7.348 p=<0.01) compared to the other two species. Additionally, *G. capensis* had significantly larger muscle volume percentages in both heads of m.

gastrocnemius (GCM: F=4.431 p=0.03, GCL: F=5.155, p=0.02) compared to both *B. suillus* and *C. h. natalensis*.

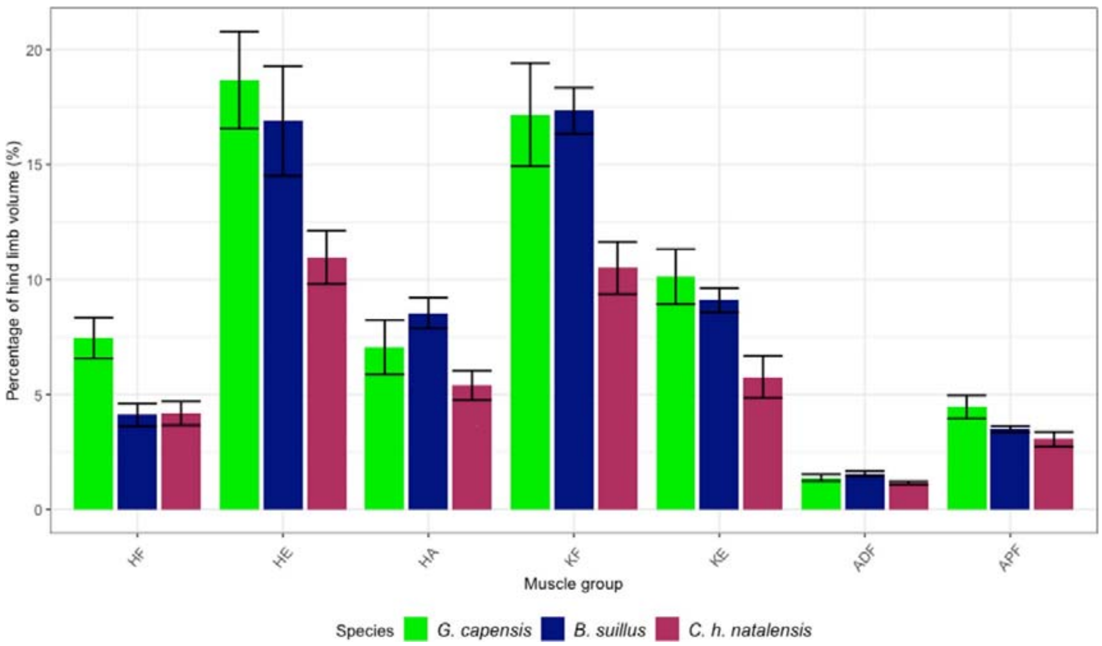

Figure 7. The mean summed percentage of the total hind limb per muscle per muscle group for *Georychus capensis*, *Bathyergus suillus* and *Cryptomys hottentotus natalensis*. The error bars denote the standard error. Muscle group abbreviations: Hip flexors (HF), hip extensors (HE), hip adductors (HA), knee flexors (KF), knee extensors (KE), ankle dorsiflexors (ADF), ankle plantar flexors (APF).

Interestingly, several muscles made up a larger percentage of the total hind limb muscle volume in *G. capensis* compared to both other species, although this was not statistically significant. These muscles were: *mm. adductor brevis*, the caudal head of *biceps femoris, semitendinosus*, *vastus intermedius* and *vastus medialis*. The *m. vastus lateralis* of *G. capensis* and the *m. gracilis anticus* of *B. suillus* had the largest muscle volume percentages of all the muscles measured, where both muscles made up more than 4% of the total hindlimb volume.

The mean summed percentage of the total hind limb volume of the hip extensor and knee flexor muscle groups of the two drumming species was greater than 15%. Furthermore, *Georychus capensis* had the largest summed percentage of the total hind limb volume in the hip flexor, hip extensor, knee extensor and ankle plantar flexor muscle groups in the three species (Figure 7).

DISCUSSION

Recently, diceCT has been used in comparative morphological studies on the masticatory muscles of African mole-rats (Cox & Faulkes, 2014, Cox et al., 2020). However, quantitative studies using this technique which also include statistical comparisons to determine morphological adaptations, are rare. The present study aimed to use diceCT scanning (Metshcer, 2009; Jeffery et al., 2011, Gignac et al., 2016) to determine volumetric comparisons of 27 muscles of the hind limb in three species of African mole-rats.

Despite the size differences between the species studied here, the present study successfully used diceCT to reveal individual muscles of the hind limb in all three species of African mole-rats. Several studies using contrast enhanced micro-CT scans of muscles used I_2KI as the contrast agent (Cox & Faulkes, 2014; Lautenschlanger, et al., 2014; Bribiesca-Contreras & Sellers, 2017; Cox et al., 2020). As expected, the I_2KI aqueous solution had a strong affinity for the muscle tissue as described by Jeffery, et al. (2011). The fact that adipose tissue and other soft tissues did not absorb the contrast agent well in the present study, allowed for clear definition of individual muscles. However, I_2KI did not allow for clear demonstration of tendons of origin or insertions, as was the case in a study on wing muscles of the sparrow hawk (*Accipiter nisus*; Bribiesca-Contreras & Sellers, 2017). An alternative staining technique namely phosphotungstic acid, which binds to collagen, was used in several studies comparing staining methods and was more successful with showing tendons of muscles (Mizutani & Suzuki, 2012; Descamps, et al., 2014). However, as the present study was more focused on determining differences in the muscle volumes between species, the phosphotungstic acid method was not used.

Apart from being able to determine volumes of muscles, the 3D reconstructions obtained from micro-CT allow for good visualization of structures which are difficult to reach during macroscopic dissections. This non-destructive technique prevents damage to the specimen and allows for the relationships between structures to be clearly apparent, especially in small specimens (Cox & Faulkes, 2014, Lautenschlager, et al., 2014; Cox et al., 2020). In the present study, the diceCT scan confirmed a single *m. gracilis* in the two drumming species as documented in Sahd et al. (2019). Furthermore, it clearly illustrated that the *m. gracilis anticus* occupied a significantly larger percentage of the total hind limb muscle volume in both drumming species compared to the non-drumming *C. h. natalensis.* In fact, even when combined, the *m. gracilis* complex (*Mm. gracilis anticus* and *posticus*) of *C. h. natalensis* had a mean total hind limb volume percentage of only 1.83%, which is still less than the volume of the singular *m. gracilis* of *G. capensis* (2.42%) and *B. suillus* (4.15%). Additionally, *m. gracilis anticus* has been postulated to play a key role in hind foot drumming as its muscle architecture parameters (fascicle length, physiological cross sectional area and muscle mass) are significantly different between *C. h. natalensis* and *G. capensis* (Sahd, et al., 2021), the latter being the fastest drumming species of the two drumming mole-rats species (Narins *et al*., 1992; Van Sandwyk & Bennett, 2005).

Several studies in humans and rats have illustrated that sustained periods of exercise result in an increase in muscle volume (Yarasheski, et al 1990; Tesch, et al, 2004). The *mm. gluteus superficialis*, *semimembranosus*, *gluteofemoralis*, *rectus femoris* and *vastus lateralis* of the two drumming species had significantly larger muscle volume percentages compared to the non-drumming *C. h. natalensis*. This may be indicative of hypertrophy of these muscles as a result of the rapid hind foot drumming observed in the drumming species (*G. capensis and B. suillus*). These particular muscles are key muscles in the extension and adduction of the hip joint as well as flexion and extension of the knee joint (Sahd, et al., 2019). As the action of hind foot drumming in these mole-rats is facilitated by the rapid flexion and extension of the hip and knee joints of a single or alternating hind limb (Randall, 2014), these muscles may play a key role in hind foot drumming. Additionally, the muscle architecture of the two drumming species studied here indicated that the hip and knee flexor and extensor muscles groups were capable of high-power output compared to *C. h. natalensis* (Sahd et al*.,* 2021).

Georychus capensis drums faster than *B. suillus,* the difference in the speed of drumming may influence the muscle volume percentages. Fast eccentric contractions (as seen during hip extension during drumming) have caused greater hypertrophy in humans than slow eccentric contractions (Farthing & Chilibeck, 2003). Additionally, the significantly larger volume percentages in *G. capensis* observed in the cranial head of *m. biceps femoris* and both heads of *m. gastrocnemius* compared to the non-drumming *C. h. natalensis,* could indicate compensation for the mechanical loading of rapid drumming resulting in enlarged muscles in *G. capensis*.

However, while not statistically significant, *B. suillus* had larger muscle volume percentages in several hip extensor and knee flexor muscles compared to *G. capensis* (except *m. vastus lateralis*; Figure 6) which could be attributed to the large size of this species. Therefore, the size difference between the species (Table 1) may have contributed to the statistical differences observed between the drumming and non-drumming species. *Bathyergus suillus* is the largest member of the family Bathyergidae (weighing up to 2 kg; Bennett et al*.,* 2009) while the small *C. h. natalensis* has a mean body mass ranging between 88 and 106 g (Jarvis & Bennett, 1991) and *G. capensis* is a medium sized species with a mean body mass of 180 g (Bennett et al., 2006). This is emphasised by significantly larger relative muscle volumes observed in *B. suillus* compared to the other two species. Additionally, the relative sizes of the hip flexor, *m. pectineus* and the hip extensor, *m. gluteus medius* were significantly larger in *B. suillus* compared to the very small *C. h. natalensis.* Therefore, the locomotory demands to move the larger hind limbs in *B. suillus* may require relatively larger hip flexor and extensor muscles to exert more force to lift their large hind limbs when manoeuvring in their burrow systems. This corresponds with the outcomes of muscle architecture of *m. gluteus medius* in *B. suillus* which indicates that it is capable of more forceful contraction than in *C. h. natalensis* (Sahd et al., 2021).

The larger muscle volume percentages observed in *B. suillus* compared to the other two species could also be influenced by the digging strategy employed by this bathyergid species. *Bathyergus suillus* is a scratch digging member of the family Bathyergidae while both *G. capensis* and *C. h. natalensis* use chisel tooth digging to expand their burrow systems (Bennett & Faulkes, 2000). The large volume of *mm. soleus* and *extensor digitorum longus* in *B. suillus* could be indicative of a hind limb stabilisation function during digging (Hildebrand, 1985; Samuels & Van Valkenburgh, 2008). This contradicts our hypothesis that the ankle dorsi-and plantar flexors of the three species would have similar muscle volume percentages and may be an adaptation for digging in *B. suillus*. Furthermore, the large *m. abductor magnus* could be used to maintain a more abducted limb position of the femur during soil excavation, similar to that observed in tenrecs (Salton & Sargis, 2009). These relatively larger muscles in *B. suillus* may provide stability and support during the torsional force exerted by the power stroke of the forelimb during scratch digging (Hildebrand, 1985).

Limitations and future directions

A limitation to this study is that two large muscles namely *mm. iliacus* and *psoas major* in the *B. suillus* specimens did not absorb I_2KI very well and were therefore excluded from the study. The I_2KI contrast agent causes significant shrinkage of the muscle tissue as illustrated by Vikteron et al. (2013) and Buytaert et al. (2014) and a correction factor was therefore applied with the assumption that all the muscles were penetrated equally by the contrast agent. The two hind foot drumming species studied in the present study are sister-genera and therefore similarities observed in the muscles of these two species may be a result of phylogenetic similarities rather than be an adaptation for hind foot drumming. Hence, further analyses on other drumming and non-drumming species of rodents are needed to confirm the preliminary conclusions derived in the present studies. In addition, future studies could make use of the information provided in the present study to create musculoskeletal simulation models in addition to electromyographical readings taken during drumming, to confirm the involvement of specific muscles during drumming.

CONCLUSION

Micro-CT scanning is becoming an invaluable part of comparative morphological studies. More recently, diceCT has allowed for the visualisation and volume determination of soft-tissue, especially muscles. Previously, gross dissections showed that the *m. gracilis* was a single muscle in the two drumming species. The 3-D CT scans confirmed this finding and additionally showed that this muscle had a statistically significant larger volume in the drumming mole-rat species compared the non-drumming species. Additionally, several hip and knee extensors had significantly larger muscle volume percentages in the two drumming species (*G. capensis* and *B. suillus*) compared to the non-drumming species thus confirming our first hypothesis. While not statistically significant, *G. capensis* had larger muscle volume percentages in several key hip and knee extensors compared to *B. suillus.* Additionally*, G capensis* had the largest summed percentage of the total hind limb volume in the hip flexor, hip extensor, knee extensor and ankle plantar flexor muscle groups in all the three species. This could be indicative of whole muscle hypertrophy in these muscles due to fast eccentric contractions generated during hind foot drumming. However, significantly larger muscle volume percentages were observed in the scratch digging *B. suillus* compared to the other two chisel tooth digging species. Moreover, while not statistically significant, *B. suillus* had larger muscle volume percentages in several hip extensor and knee flexor muscles compared to *G. capensis* (except for *m. vastus lateralis*). These differences may be attributed to the relatively large size of this species but could also be influenced by the scratch digging, burrowing technique used by *B. suillus*. Therefore, while the action of hindfoot drumming seems to influence certain key muscle volumes, digging strategy and body size may also play a role.

ACKNOWLEDGEMENTS

The authors thank Prof Martin Kidd for assistance with the statistical analysis and the team at the CAF micro-CT facility for their help with the scans and reconstructions. The financial assistance of the National Research Foundation (NRF) and SARChi Mammal Behavioural Ecology and Physiology (Grant number 64756) towards this research is hereby acknowledged. Opinions expressed and conclusions arrived at, are those of the authors and are not necessarily to be attributed to the NRF.

AUTHOR CONTRIBUTIONS

Lauren Sahd prepared the samples, performed the analysis and drafted the manuscript. Nigel Bennett provided the samples and funding, and edited the manuscript. Sanet Kotzé was the principal investigator, designed the project, edited the manuscript, and provided funding.

Author ORCID IDs
Lauren Sahd: https://orcid.org/0000-0002-6854-6996
Nigel Bennett: https://orcid.org/0000-0001-9748-2947
Sanet Kotzé: https://orcid.org/0000-0003-0853-2178

REFERENCES

Bennett, N.C. & Faulkes, C.G. 2000. *African mole-rats: Ecology and Eusociality.* Cambridge: Cambridge University Press.

Bennett, N.C. & Jarvis, J.U.M., 1988. The reproductive biology of the Cape mole-rat, *Georychus capensis* (Rodentia, Bathyergidae). *Journal of Zoology*, 214: 95-106.

Bennett, N.C., Maree, S. & Faulkes, C.G. 2006. *Georychus capensis. Mammalian Species* 799: 1-4.

Bennett, N.C., Taylor, P.J. & Aguilar, G.H. 1993. Thermoregulation and metabolic acclimation in the Natal mole-rat (*Cryptomys hottentotus natalensis*) (Rodentia: Bathyergidae). *Zeitschrift fur Saugtierkunde* 58: 362-367.

Bishop, P.J., Michel, K.B., Falisse, A.,et al., 2021. Computational modelling of muscle fibre operating ranges in the hindlimb of a small ground bird (*Eudromia elegnans*), with implications for modelling locomotion in extinct species. *PLoS Computational Biology* 17: e100884.

Bribiesca-Contreras, F. & Sellers, W.I. 2017. Three-dimensional visualisation of the internal anatomy of the sparrowhawk (*Accipiter nisus*) forelimb using contrast-enhanced micro-computed tomography. *PeerJ* 5: e3039.

Buytaert, J., Goyens, J., De Greef, D., Aerts, P & Dirckx, J. 2014. Volume shrinkage of bone, brain and muscle tissue in sample preparation for micro-CT and light sheet fluorescence microscopy. *Microscopy and Microanalysis* 20: 1208-1217.

Charles, J.P., Cappellari, O., Spence, A.J., Hutchinson, J.R. & Wells, D.J. 2016. Musculoskeletal geometry, muscle architecture and functional specialisations of the mouse hindlimb. *PLoS ONE* 11: e0147669.

Collings, A.J. & Richards, C,T. 2019. Digital dissection of the pelvis and hindlimb of the red-legged running frog, *Phlyctimantis maculatus,* using Diffusible Iodine Contrast Enhanced computed microtomography (DICE μCT). *PeerJ* 7: e7003

Cox, P.G. & Faulkes, C. 2014. Digital dissection of the masticatory muscles of the naked mole-rat, *Hetercephalus glaber* (Mammalia, Rodentia). *Peer J* 2: e448.

Cox, P.G., Faulkes, C. & Bennett, N.C. 2020. Masticatory musculature of the African mole-rats (Rodentia: Bathyergidae). *PeerJ* 8: e8847.

Degenhardt, K. & Wright, A. 2010. Rapid 3D phenotyping of cardiovascular development in mouse embryos by micro-CT with iodine staining. *Circulation: Cardiovasc Imaging* 33: 314–322.

Descamps, E., Sochacka, A., De Kegel, B., Van Loo, D., Van Hoorebeke, L. & Adriaens, D. 2014. Soft tissue discrimination with contrast agents using micro-CT scanning. *Belgian Journal of Zoology* 144: 20-40.

Dickinson, E., Atkinson, E., Meza, A., Kolli, S., Deutsch, A.R., Burrows, A.M. & Hartstone-Hart, A. 2020a. Visualization and quantification of mimetic musculature via DiceCT. *PeerJ* 8:e9343 https://doi.org/10.7717/peerj.9343

Dickinson, E., Basham, C., Rana, A. & Hartstone-Rose, A. 2019. Visualization and quantification of digitally dissected muscle fascicles in the masticatory muscles of

Callithrix jacchus using nondestrcutive diceCT. *The Anatomical Record* 302: 1891-1900.

Dickinson, E., Kolli, S., Schwenk, A., Davis, C.E. & Hartstone-Rose, A. 2020b. DiceCT analysis of the extreme gouging adaptations within the masticatory apparatus of the aye-aye (*Daubentonia madagascariensis*) *The Anatomical Record* 303: 282-294*.*

Du Plessis, A., le Roux, S.G. & Guelpa, A. 2016. The CT scanner facility at Stellenbosch University: An open access X-ray computed tomography laboratory. *Nuclear Instruments and Methods in Physics Research B* 384: 42-49.

Farthing, J.P. & Chilibeck, P.D. 2003. The effects of eccentric and concentric training at different velocities on muscle hypertrophy. *European Journal of Applied Physiology* 89: 578-586.

Ferreira-Cardoso, S., Fabre, P., de Thoisy, B., Delsuc, F. & Hautier, L. 2020. Comparative masticatory myology in anteaters and its implications for interpreting morphological convergence in myrmecophagous placentals. *PeerJ* 8: e9690 https://doi.org/10.7717/peerj.9690.

Gignac, P.M., Kley, N.J., Clarke, J.A. et al. 2016. Diffusible iodine-based contrast-enhanced computed tomography (diceCT): an emaerging tool for rapid high-resolution, 3-D imaging of metazoan soft tissues. *Journal of Anatomy* 228: 889-909.

Hart, L., O'Riain, M.J., Jarvis, J.U.M. & Bennett, N.C. 2006. Is the Cape dune mole-rat, *Bathyergus suillus* (Rodentia: Bathyergidae), a seasonal or aseasonal breeder? *Journal of Mammalogy* 87: 1078-1085.

Hildebrand, M. 1985. Digging of quadrupeds. In Hildebrand, M., Bramble, D.M., Liem, K.F. & Wake, D.B. (eds.) *Functional vertebrate morphology*. Cambridge: Belknap Press of Harvard University. 90–108.

Jeffery, N.S., Stephenson, R.S., Gallagher, J.A., Jarvis, J.C. & Cox, P.G. 2011. Micro-computed tomography with iodine staining resolves the arrangement of muscle fibres. *Journal of Biomechanics* 44: 189-192.

Klinkhamer, A.J., Wilhite, D.R., White, M.A. & Wroe, S. 2017. Digital dissection and three-dimensional interactive models of limb musculature in the Austrailn esturine crocodile (*Croodylus porosus*). *PLos One* 12: e0175079.

Lacey, E.A., Patton, J.L. & Cameron, G.N. (eds) *Life underground: The Biology of Subterranean Rodents.* Chicago: The University of Chicago Press.

Lautenschlanger, S., Bright, J.A. & Rayfield, E.J. 2014. Digital dissection- using contrast-enhanced computed tomography scanning to elucidate hard- and soft-tissue anatomy in the Common Buzzard *Buteo buteo*. *Journal of Anatomy* 224: 412-431.

Mason, M.J. & Narins, P.M. 2010. Seismic sensitivity and communication in subterranean mammals In: O'Connell-Rodwell, C.E. (ed) *The Use of Vibrations in Communication: Properties, Mechanisms and Function across Taxa*. Transworld Research Network, Kerala: 121-139.

Metscher, B.D. 2009. MicroCT for comparative morphology: simple staining methods allow high-contrast 3D imaging of diverse non-mineralized animal tissues. *BMC Physiology* 2009: 9-11.

Mizutani, R. & Suzuki, Y. 2012. X-ray microtomography in biology. *Micron* 43:104-115.

Narins, P.M., Reichman, O.J., Jarvis, J.U.M. & Lewis, E.R. 1992. Seismic signal transmission between burrows of the Cape mole-rat, *Georychus capensis. Journal of Comparative Physiology A* 170: 13-21.

Nowak, R.M. & Paradiso, J.L. 1983. *Walker's Mammals of the World.* 4th edition. London: The Johns Hopkins University Press.

R Core Team. 2013. R: A language and environment for statistical computing. R Foundation for Statistical Computing, Vienna, Austria. URL http://www.R-project.org/.

Randall, J.A. 2014. Vibrational communication: spiders to kangaroo rats. In: Witzany, G. (ed) *Biocommunication of Animals.* Springer, Dordrecht: 103-133.

Sahd, L., Bennett, N.C. & Kotzé, S.H. 2019. Hind foot drumming: morphological adaptations of the muscles and bones of the hind limb in three African mole-rat species. *Journal of Anatomy* 235: 811-842. doi: 10.1111/joa.13028.

Sahd, L., Bennett, N.C. & Kotzé, S.H. 2021. Hind foot drumming: Muscle architecture of the hind limb in three Bathyergidae species. *Journal of Mammalian Evolution* 28: 511-525.

Santana, S.E. 2018. Comparative anatomy of bat jaw musculature via diffusible iodine-based contrast-enhanced computed tomography. *The Anatomical Record* 301: 267-278.

Sherman, P.W., Jarvis, J.U.M. & Alexander, R.D. 1991. *The Biology of the Naked Mole-rat*. Princeton: Princeton University Press.

Sullivan, S.P., McGechie, F.R., Middleton, K.M. & Holliday, C.M. 2019. 3D muscle architecture of the pectoral muscles of European Starling (*Sturnus vulgaris*). *Intergrative Organismal Biology* Bennett, N.C. & Jarvis, J.U.M., 1988. The reproductive biology of the Cape mole-rat, *Georychus capensis* (Rodentia, Bathyergidae). *Journal of Zoology*, 214: 95-106.

Tesch, P.A., Ekberg, A., Lindquist, D.M. & Trieschmann, J.T. 2004. Muscle hypertrophy following 5-week resistance training using a non-gravity-dependent exercise system. *Acta Physiologica Scandinavica* 180: 89-98.

Van Sandwyk, J.H.d.T. & Bennett, N.C. 2005. Do solitary seismic signalling Cape mole-rats (*Georychus capensis*) demonstrate spontaneous or induced ovulation? *Journal of Zoology London* 267: 75-80.

Vickerton, P.., Jarvis, J & Jeffery, N. 2013. Concentration-dependent specimen shrinkage in iodine-enhanced microCT. *Journal of Anatomy* 223: 185-1933.

Wickham, H. 2016. *ggplot2: Elegant Graphics for Data Analysis*. Springer-Verlag, New York

Yarasheski, K.E., Lemon, P.W. & Gilloteaux, J. 1990. Effect of heavy-resistance exercise training on muscle fiber composition in young rats. *Journal of Applied Physiology* 69: 434-437.